

This article was downloaded by: [Tomsk State University of Control Systems and Radio]

On: 20 February 2013, At: 12:37

Publisher: Taylor & Francis

Informa Ltd Registered in England and Wales Registered Number: 1072954

Registered office: Mortimer House, 37-41 Mortimer Street, London W1T 3JH, UK



Molecular Crystals and Liquid Crystals

Publication details, including instructions for authors and subscription information:

<http://www.tandfonline.com/loi/gmcl16>

Charge and Spin Density Waves in Charge-Transfer Solids

S. Mazumdar^a, S. N. Dixit^b & A. N. Bloch^c

^a Center for Nonlinear Studies, Los Alamos National Laboratory, Los Alamos, New Mexico, U.S.A.

^b Noyes Laboratory for Chemical Physics, California Institute of Technology, Pasadena, California, U.S.A.

^c Exxon Research and Engineering Company, Annandale, New Jersey, U.S.A.

Version of record first published: 17 Oct 2011.

To cite this article: S. Mazumdar, S. N. Dixit & A. N. Bloch (1985): Charge and Spin Density Waves in Charge-Transfer Solids, *Molecular Crystals and Liquid Crystals*, 120:1, 35-42

To link to this article: <http://dx.doi.org/10.1080/00268948508075756>

PLEASE SCROLL DOWN FOR ARTICLE

Full terms and conditions of use: <http://www.tandfonline.com/page/terms-and-conditions>

This article may be used for research, teaching, and private study purposes. Any substantial or systematic reproduction, redistribution, reselling, loan, sub-licensing, systematic supply, or distribution in any form to anyone is expressly forbidden.

The publisher does not give any warranty express or implied or make any representation that the contents will be complete or accurate or up to date. The accuracy of any instructions, formulae, and drug doses should be

independently verified with primary sources. The publisher shall not be liable for any loss, actions, claims, proceedings, demand, or costs or damages whatsoever or howsoever caused arising directly or indirectly in connection with or arising out of the use of this material.

CHARGE AND SPIN DENSITY WAVES IN CHARGE-TRANSFER SOLIDS

S. MAZUMDAR

Center for Nonlinear Studies, Los Alamos National Laboratory,
Los Alamos, New Mexico, U.S.A.

S. N. DIXIT

Noyes Laboratory for Chemical Physics, California Institute
of Technology, Pasadena, California, U.S.A.

A. N. BLOCH

Exxon Research and Engineering Company, Annandale, New Jersey,
U.S.A.

Abstract It is shown that the strengths and periodicities of charge and spin density waves in the organic charge-transfer solids depend very strongly on the degree of charge transfer ρ . We thereby explain both the appearance of the $4k_F$ charge density wave near $\rho = 0.5$ and its nonexistence for $\rho \geq 0.6$, while for ρ slightly larger (but not smaller) than 0.5 we predict a new kind of Coulomb-induced defect.

The role of Coulomb correlations in the organic charge transfer solids has been a source of continuing controversy, primarily because the accepted signatures of strong Coulomb correlations, enhanced magnetic susceptibility and the $4k_F$ instability (k_F = Fermi wavevector in the noninteracting model) occur in some materials even as they are absent in others with very similar molecular components. We have recently shown² that the origin of this controversy lies in the neglect of all intermolecular Coulomb interactions in previous theoretical descriptions of these materials. Specifically, within the proposed Hubbard Hamiltonian for these systems, a uniform behavior for the entire family of charge transfer solids is expected if the magnitude of U/t , where U and t are the Hubbard parameters for the on-site electron correlation and the nearest neighbor hopping integral, is nearly the same within the family. Similar uniform behavior is again expected if the intersite interactions are included but only the $U = \infty$ limit of such an extended Hubbard model is considered.³ As we have recently shown² in a calculation of temperature dependent magnetic susceptibilities as a function of the degree of charge transfer ρ , only when the intersite interactions are included explicitly and all terms in the Hamiltonian are kept finite, a

strong and systematic ρ -dependence is found. Magnetic susceptibility can still be described within a Hubbard model with an effective on-site repulsion U_{eff} , but now U_{eff} is ρ -dependent and is large near $\rho \sim 0.5$ but small near $\rho \sim 0.75$. Detailed comparison with real systems shows that the magnetic susceptibility of the entire family obeys our theoretical prediction.²

The parameter U_{eff} is a measure only of the normalized probability of double occupancy $g(0) = \langle n_{i\sigma} n_{i\bar{\sigma}} \rangle / \langle n_{i\sigma} \rangle \langle n_{i\bar{\sigma}} \rangle$, where $n_{i\sigma}$ is the number operator (with spin σ) for site i . A small $g(0)$ is both necessary and sufficient for enhanced susceptibility, while it is a necessary but not sufficient condition for the $4k_F$ charge density wave (hereafter CDW). For more complete understanding of the ρ -dependence of CDW behavior, we need to know the full pair correlation function $g(i-j) = \langle n_{i\sigma} n_{i+j\sigma} \rangle$, where $n_i = \sum_{\sigma} n_{i\sigma}$. It is

the purpose of the present paper to develop real space concepts of broken symmetry that are valid for all broken symmetry solutions ($2k_F$ and $4k_F$ CDW and SDW), and all values of correlation parameters and ρ . The band picture is not valid for strongly correlated systems, while the real space ideas of broken symmetry remain unchanged for all values of the correlation parameters. Similar concepts have recently been successfully applied to the bond-alternation problem in a correlated half-filled band, both without⁴ and with⁵ site energy differences. We show here that a strong $4k_F$ CDW can occur only if $\rho < 2/3$, while for still larger ρ only a weak $2k_F$ CDW is expected. In addition, for ρ slightly larger than 0.5, the $4k_F$ CDW gives way to a dimerization plus a new Coulomb-induced defect. Our theory rationalizes the full range of $4k_F$ behavior observed experimentally, and specifically the sequence of instabilities found in the variable ρ -system (NMP)_x(Phen)_{1-x}TCNQ.

We consider the extended Hubbard Hamiltonian,

$$H = H_{e-e} + H_t \quad (1a)$$

$$H_{e-e} = U \sum_i n_{i\uparrow} n_{i\downarrow} + \sum_{i,j} V_{ij} n_i n_j \quad (1b)$$

$$H_t = t \sum_i (a_{i0}^+ a_{i+1,0} + a_{i+1,0}^+ a_{i0}) \quad (1c)$$

where $a_{i\sigma}$ annihilates an electron of spin σ on site i , U and t are the usual Hubbard parameters, and all intersite interactions V_j beyond V_2 are neglected and even V_2 is small. The discussion below is valid for the range $4 \leq U/t \leq 15$, $2 \leq v_1/t \leq 4$ and $V_1 \leq U/2$, and we believe that the present arguments and results are applicable to the complete family of charge transfer solids.

The ground state solutions of Eq. 1 can be expressed as weighted sums of real-space many-electron configurations. Among these the ones which favor most strongly a CDW of period Q are those yielding the largest eigenvalues of the structure factor operator,

$$\hat{S}(q) = N^{-1} \sum_{\ell, j} n_{\ell} n_{j+\ell} e^{iqj} \quad (2)$$

at $q = Q$. For all ρ , each such configuration is completely equivalent to all other configurations generated from it by a rigid translation of all electrons by an integral number of lattice sites. When weighted equally, the set of equivalent configurations contribute to a uniform state. Only when they are weighted unequally do they break symmetry and make a periodic contribution to the measured structure factor, the expectation value of Eq. (2).

$$S(q) = N^{-1} \sum_{\ell, j} \langle n_{\ell} n_{\ell+j} \rangle e^{iqj} \quad (3)$$

A set of equivalent configurations can be unequally weighted only if they are separated from one another by a substantial barrier in energy. For example, according to Eq. (1), it is physically possible to pass from one configuration to its phase-shifted equivalent by successive nearest-neighbor one-electron transfers expressed by repeated application of the transfer operator H_t . All possible "paths" between the extreme configurations can be generated in this manner, and perfect resonance (in the chemical sense) requires that the energy barriers along these paths be small, while a large barrier can give rise to broken symmetry. The barrier to resonance has a one-electron kinetic energy part which increases with the lengths of the paths,^{4,5} as well as a coulomb part which depends on the difference of the diagonal matrix elements of H_{e-e} for configurations along any path. The coulomb barrier is positive if intermediate configurations along a path have larger potential energies than the starting and final configurations, and negative otherwise.^{4,5}

We now observe that all configurations contributing to a given broken symmetry lie along paths between the set of configurations which give the largest eigenvalues in Eq. (2). Therefore, in order to discuss the strength of a given instability, it is sufficient to confine our attention to these extreme configurations alone. In this way we are able to determine the correlation effects upon instabilities by simple inspection.

We choose the four cases $\rho = 0.5, 0.6, 2/3$ and 0.8 for illustration, but emphasize that our arguments are valid for all ρ . In Table 1 we have presented the extreme configurations for these ρ .

Here configurations (i), (iii), (vi) and (ix) (and all others reached by a phase shift) favor the $2k_F$ CDW most strongly, while configurations (ii), (iv), (vii) and (x) favor the $4k_F$ CDW most strongly. The significance of configurations (v) and (viii) will be discussed later. Notice that in all cases extreme configurations which favor the $4k_F$ CDW most strongly are the Wigner crystal configurations³ for these ρ . For $\rho = 2/3$, $2k_F = 4k_F$, but for comparison with other ρ we will consider the periodicity to be $2k_F$ if the wavefunction is dominated by (vi), and $4k_F$ if it is dominated by (vii).

TABLE I Extreme configurations that favor periodicities $2k_F$, $4k_F$ and π/a for several different ρ (see text).

ρ	Extreme configurations									
0.5	(i)	2	0	0	0	2	0	0	0	2
	(ii)	1	0	1	0	1	0	1	0	1
0.6	(iii)	2	0	0	0	2	0	0	2	0
	(iv)	1	0	1	1	0	1	0	1	1
	(v)	1	0	1	0	1	1	1	0	1
2/3	(vi)	2	0	0	2	0	0	2	0	0
	(vii)	1	1	0	1	1	0	1	1	0
	(viii)	1	0	1	1	1	0	1	0	1
0.8	(ix)	2	0	2	0	0	2	0	2	0
	(x)	1	1	1	1	0	1	1	1	1

From the nature of the extreme configurations in Table I and the paths⁴ connecting them, we then arrive at the following conclusions.

(1) Extreme configurations favoring the $2k_F$ CDW have the largest possible number of double occupancies, so that the Coulomb barriers along paths connecting these are $-U$, $-2U$, ... etc. Positive U therefore will suppress the $2k_F$ CDW for any ρ .

(2) For the $4k_F$ CDW in $\rho = 0.5$, paths connecting the two extreme configurations can have a zero correlation barrier for $U > 0$ but $V_1 = 0$. Only for $V_1 > 0$ we expect the $4k_F$ CDW, which should persist for $V_2 \leq V_1/2$.

(3) For $0.5 < \rho \leq 2/3$, two different kinds of extreme configurations involving single occupancies only are possible. The former favor periodicity $4k_F$ most strongly, while the latter favor dimerization with periodicity π/a most strongly and are obtained by singly occupying the forbidden sites in configuration (ii).

Configurations (v) and (viii) correspond to such "defect" configurations for $\rho = 0.6$ and $2/3$ in Table I. The actual periodicity of the ground state CDW depends on whether the ground state has greater contribution from the extreme $4k_F$ configurations or the "defect" configurations. For $V_2 = 0$, the matrix elements of H^{e-e} are equal for both kinds of extreme configurations, but while the "defect" configurations have low energy excitations at $U - 2V_1$, in which the central electron in a sequence of three occupied sites hops to one of its neighbors, the corresponding excitations in the $4k_F$ configurations that lead to double occupancy cost $U - V_1$. Configuration interaction therefore favors the defect configuration and we expect periodicity π/a to dominate over $4k_F$. For $V_2 \neq 0$, the matrix element of H^{e-e} is smaller for the $4k_F$ configuration, so that once V_2 exceeds a critical value the stabilization due to configuration interaction will not be sufficient to prevent the crossover to $4k_F$.

(4) For $\rho < 0.5$ the "defect" configurations contain sequences of three empty sites, so that stabilization of periodicity π/a by configuration interaction is absent. We therefore do not expect periodicity π/a in $\rho < 0.5$.

(5) For $\rho > 2/3$, the addition of a single electron leads to a long sequence of singly occupied sites, as may be seen from both (vii) and (viii) in Table I. The implication of this is that paths between extreme configurations can now have zero correlation barrier even with $V_2 \neq 0$. This may be further seen from configuration (x), where allowed hops (i.e., those not leading to double occupancies) again cost zero energy. Thus within this region we do not expect a strong $4k_F$ CDW. On the other hand, starting from $\rho = 2/3$, the maximum distance between a pair of double occupancies in extreme configurations favoring the $2k_F$ CDW is three lattice sites, so that both V_1 and V_2 can add to the barrier to resonance between these extreme configurations. A weak $2k_F$ CDW may therefore be expected here.

The above conclusions are substantiated by exact numerical calculations on periodic rings of $N = 10-12$ sites. Careful comparisons to both smaller and larger systems were made to verify that finite size effects are small. Our results are in complete agreement with previous Monte Carlo simulations for the special cases $\rho = 0.5$ and 0.6 .⁸ In Fig. 1(a) we have plotted $S(q)$ against q for five different ρ , for $U = 7\sqrt{2}t$, $V_1 = V_2 = 0$. As expected from our discussion above, the $2k_F$ CDW has been suppressed but there is no recognizable peak at $4k_F$. Our results for $U = 7\sqrt{2}t$, $V_1 = 3\sqrt{2}t$, $V_2 = 0$ are shown in Fig. 1(b). A strong peak at $4k_F = \pi/a$ is now seen for $\rho = 0.5$, but for $\rho = 0.6$ and $2/3$ the peaks in $S(q)$ also occur at π/a instead of at the proper $4k_F$ wavevectors. Notice, however, that $S(q)$ for $\rho = 0.4$ peaks at $4k_F$, thus demonstrating that this is not a simple commensurability

effect. Similar results are also obtained for $\rho = 0.43$ (not shown here), for which the calculations were performed for even larger size ($N = 14$). For $\rho = 0.8$, we find only a weak $2k_F$ CDW, as predicted. Only when a large enough V_2 is added to the Hamiltonian ($V_2 > 0.4\sqrt{2}t$) the peaks in $S(q)$ for $\rho \leq 0.6$ and $2/3$ shift to $4k_F$, as is seen in Fig. 1(c), where we have plotted out results for the above U and V_1 and $V_2 = \sqrt{2}t$.

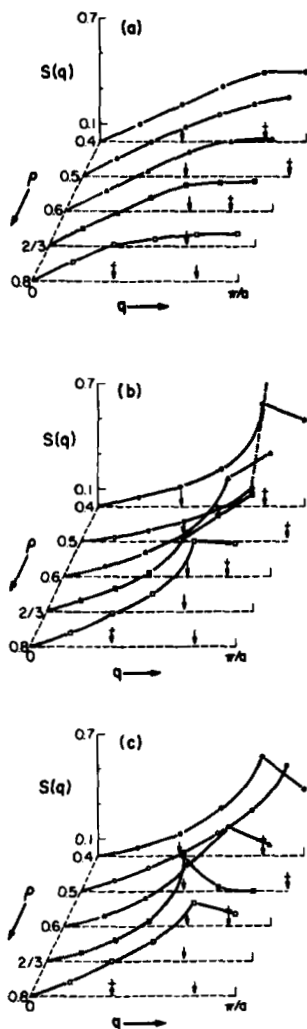


FIGURE 1 $S(q)$ for five different ρ at $U = 7\sqrt{2}t$, for the three cases, (a) $V_1 = V_2 = 0$, (b) $V_1 = 3\sqrt{2}t, V_2 = 0$, and (c) $V_1 = 3\sqrt{2}t, V_2 = \sqrt{2}t$. The arrows and hatched arrows on the q -axes give the $2k_F$ and $4k_F$ wavevectors respectively for the corresponding ρ . $S(\pi/a)$ for $\rho = 0.5$ is much larger (~ 1.7) than all other values shown in Figure b.

We believe the present model is directly applicable to organic charge transfer solids in which the $4k_F$ instability does not occur for $\rho \gtrsim 0.6$. The critical ρ of $2/3$ found here will be pushed to smaller values in real systems due to interchain Coulomb interactions, as $4k_F$ CDWs in neighboring chains can be perfectly off-phase only in $\rho = 0.5$, as may be seen from Table I, while beyond this the extent to which interchain Coulomb interactions oppose the $4k_F$ CDW increases with ρ . The $2k_F$ instability in $\rho > 2/3$ in real systems will have considerable intersite CDW and SDW character. We have not presented our results for SDWs here, but in general the strength of the SDW increases with U . For the extended Hubbard model, the strength is largest for $\rho = 0.5$ and decreases with ρ until $\rho \sim 0.75$ is reached, as might be expected from the calculated behavior of $g(0)$ and our previous calculations of magnetic susceptibility.²

The behavior predicted from Eq. (1) is seen most clearly in the variable ρ system (NMP)_x(Phen)_{1-x}TCNQ, in which for $x \rightarrow 0.5$ ($\rho \sim 0.5$) a $4k_F$ CDW is observed, while for $x \rightarrow 1$ ($\rho \sim 2/3$) only a $2k_F$ CDW is found. In addition, for $0.5 < x < 0.56$, the diffuse x-ray scattering wavevector stays fixed at $\frac{1}{2}g = \pi/a$, and this has been explained within a soliton mechanism⁶ that assumes $U \rightarrow \infty$, $V_1 = 0$. As shown here, a very different mechanism for this behavior is possible. Addition of a single electron to $\rho = 0.5$ generates a "trimer", a sequence of three singly occupied sites.³ A nearest neighbor hop leads to dissociation of the trimer into two "dimers", or a nearest neighbor pair of occupied sites, while a series of such hops leads finally to the configuration that favors $4k_F$ most strongly. As discussed above and seen in Fig. 1(b), the dimer pairs can be bound by configuration interaction, and this can lead to the observed behavior in (NMP)_x(Phen)_{1-x}TCNQ. For ρ sufficiently larger than 0.5, the mean distance between dimer pairs in the $4k_F$ configuration is small, so that larger and larger binding energy between dimers is required to prevent a crossover to $4k_F$ from π/a . For a fixed U/V_1 (fixed binding energy), we then expect a crossover at a suitable ρ which is a function of all the parameters. The predictions of the present mechanism are different from those of the soliton mechanism in two ways, (i) for $\rho < 0.5$ we do not expect the x-ray scattering wavevector to remain fixed at π/a , while perfect symmetry around 0.5 is expected within the soliton mechanism, (ii) within the present mechanism the gap in the electronic spectrum for $x \rightarrow 0.5$ is predominantly due to V_1 (more precisely $V_1 - 2V_2$) while within the previous mechanism this is a Peierls gap. Optical measurements¹⁰ in (NMP)_x(Phen)_{1-x}TCNQ reveal an absorption edge at $\sim 1000 \text{ cm}^{-1}$ and a peak at $\sim 3500 \text{ cm}^{-1}$, and ρ -dependent "mid-gap" absorptions are expected as ρ is increased from 0.5 within the soliton mechanism. Within the extended Hubbard Hamiltonian no additional low frequency absorptions are expected.¹¹ The present data¹⁰ do not show strong ρ -dependence and thus would

tend to support our model. We emphasize, however, that our model does not exclude the more conventional soliton but simply points out that an alternate explanation for the present observations are possible, and further experiments are necessary to distinguish between the two models.

To conclude, the observed differences in the charge transfer solids are not due to variable correlation parameters, but are expected from Eq. (1). While several mechanisms for scattering at $4k_F$ have been postulated, the present model is the only one that predicts both the existence and the non-existence of a strong $4k_F$, with the bandfilling emerging as a new and important parameter.

ACKNOWLEDGMENTS

We are grateful to Dr. A. J. Epstein and Dr. D. B. Tanner for several useful discussions on the optical properties of $(NMP)_x(Phen)_{1-x}TCNQ$.

REFERENCES

1. See, for example, Proc. Int. Conf. on Physics and Chemistry of Synthetic Metals, J. Phys. C3 (1983).
2. S. Mazumdar and A. N. Bloch, Phys. Rev. Lett. 50, 207 (1983); A. N. Bloch and S. Mazumdar in ref. 1, p. 1273.
3. J. Hubbard, Phys. Rev. B17, 494 (1978).
4. S. Mazumdar and S. N. Dixit, Phys. Rev. Lett. 51, 292 (1983); Phys. Rev. B29, 1824 (1984).
5. S. Mazumdar and S. N. Dixit, Phys. Rev. B29, 2317 (1984).
6. A. J. Epstein et al., Phys. Rev. Lett. 47, 741 (1981) and 49, 1037 (1982).
7. J. E. Hirsch and D. J. Scalapino, Phys. Rev. Lett. 50, 1168 (1983); Phys. Rev. B27, 7169 (1983).
8. J. E. Hirsch and D. J. Scalapino, Phys. Rev. B29, 5554 (1984).
9. M. J. Rice and E. J. Mele, Phys. Rev. B25, 1339 (1982).
10. A. J. Epstein, private communications. See also present proceedings.
11. S. Mazumdar and Z. G. Soos, Phys. Rev. B23, 2810 (1981).